

Effect of whole-body vibration on human body while crossing speed hump

Nitin Baburao Shelke

A Thesis Submitted to
Indian Institute of Technology Hyderabad
In Partial Fulfillment of the Requirements for
The Degree of Master of Technology



Department of Mechanical and Aerospace Engineering

June 2016

Declaration

I declare that this written submission represents my ideas in my own words, and where ideas and words of others have been included, I have adequately cited and referenced the original sources. I also declare that I have adhered to all principles of academic honesty and integrity and have not misinterpreted or fabricated or falsified any idea/data/fact/source in my submission. I understand that any violation of the above will be a cause for disciplinary action by the Institute and can also evoke penal action from the sources that have thus not been properly cited, or from whom proper permission has not been taken when needed.



(Signature)

NITIN BABURAO SHELKE

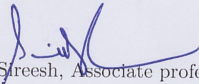
(Student Name)

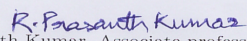
MEK4MTECH 11032

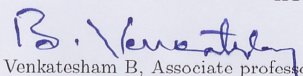
(Roll No.)

Approval Sheet

This thesis entitled " Effect of whole body vibration on human body while crossing speed hump" by Nitin Baburao Shelke is approved for the degree of Master of Technology from IIT Hyderabad.


Dr. S Sreesh, Associate professor
(—————) Examiner
Dept. of Civil Engineering
IITH


Dr. R Prasanth Kumar, Associate professor
(—————) Adviser
Dept. of Mechanical and Aerospace Engineering
IITH


Dr. Venkatesham B, Associate professor
(—————) Internal examiner
Dept. of Mechanical and Aerospace Engineering
IITH

Acknowledgements

I would like to express my gratitude towards my adviser Dr. R Prasanth Kumar for his valuable guidance, motivation and constant support in completion of this project. It was a great honour for me to pursue my masters under his supervision. I would like to express my special gratitude and thanks to class mates and friends who have willingly helped me out of their abilities.

Dedication

Dedicated to
My beloved family

Abstract

In medical point of view study of whole-body vibration is very important because whole-body vibrations (WBV) has adverse effects on ride comfort and human health. Major back pain problems arises due to long term exposure to vibration, also it can induce degenerate changes in lumber spine. ISO 2631-5:2004 is used to evaluate the effect of long-term exposure to the WBV on human health. It defines a method of quantifying whole-body vibration containing multiple shocks (such as bumpy rides) in relation to human health. It uses peak vibration (shock) values to predict compression stress in the spine, and reports equivalent daily static compression dose, S_{ed} . The results show high S_{ed} values with high health risks even at low speeds. Therefore to investigate the effect of whole body vibration on human body a two dimensional combined multibody model of half car and human body is build which allows the determination of joint reaction forces at each body joint and adverse effect of whole body vibration on human spine. Half car model consist of sprung mass, unsprung mass and spring-damper(suspension). Half car model has four degrees of freedom. Human hody model consists of rigid bodies which represent major human body segments and structured as linked open-tree multibody system. For vertical excitation speed hump of various profiles are used. Various models of human body and half car are used to study the effect of WBV on human body. The intensity of WBV is reduced by seat inclination.

Contents

Declaration	ii
Approval Sheet	iv
Acknowledgements	v
Abstract	vii
Nomenclature	ix
1 Introduction and Literature Review	3
1.1 Introduction	3
1.2 Introduction to whole-body vibration	3
1.3 Literature review	4
1.4 Motivation, scope and objectives	5
1.5 Thesis layout	5
2 Evaluation of Effect of Whole-Body Vibrations on Human Body	7
2.1 Evaluation according to ISO 2631-5:2004	7
2.2 Calculation of acceleration dose and daily equivalent static compression dose	8
2.3 Speed Hump	10
2.3.1 Classification of speed hump	10
2.4 Summary	12
3 Half Car Models and Analysis	13
3.1 6 DOF Half car model introduction	13
3.1.1 6 DOF half car model parameters	14
3.1.2 Equations of motion for 6 DOF half car model	15
3.2 6 DOF half car model in ADAMS/View	16
3.3 Validation of 6 DOF model with ADAMS	16
3.4 Daily equivalent static compression dose	17
3.5 Inclined 6 DOF half car model	18
3.5.1 Effect of seat inclination on acceleration	19
3.5.2 Effect of seat inclination on daily equivalent static compression dose	21
3.6 5 DOF Half car model introduction	23
3.6.1 5 DOF half car model parameters	24
3.6.2 Equations of motion for 5 DOF half car model	25
3.7 5 DOF Half car model in ADAMS/View	25

3.8	Validation of 5 DOF model with ADAMS	26
3.9	Daily equivalent static compression dose	28
3.10	Summary	29
4	Human Body model and Analysis	30
4.1	Introduction to human body	30
4.1.1	Human body parameters	31
4.2	Combined vehicle and human body model in ADAMS/View	31
4.3	Comparison of joint reaction forces	32
4.4	Summary	34
5	Conclusions and Recommendations	35
5.1	Conclusions	35
5.2	Recommendations	35
	References	36

List of Figures

2.1	Flow chart for the assessment of adverse health effect	9
2.2	Flat platform	11
2.3	Rounded Profile	11
3.1	6 DOF Half Car Model	14
3.2	6 DOF Half Car Model in ADAMS/View	16
3.3	Validation of displacement while passing over Rounded Profile	17
3.4	Validation of velocity while passing over Rounded Profile	17
3.5	Variation of daily equivalent static compression dose with velocity	18
3.6	Inclined 6 DOF Half Car Model in ADAMS/View	19
3.7	Effect of seat inclination on acceleration of passenger1	20
3.8	Effect of seat inclination on acceleration of passenger2	20
3.9	Variation of daily equivalent static compression dose with velocity over rounded profile	21
3.10	Variation of daily equivalent static compression dose with velocity over flat platform	22
3.11	Variation of daily equivalent static compression dose with velocity over rounded profile	22
3.12	Variation of daily equivalent static compression dose with velocity over flat platform	23
3.13	5 DOF Half Car Model	24
3.14	5 DOF Half Car Model in ADAMS	26
3.15	Validation of displacement while passing over Rounded Profile	27
3.16	Validation of velocity while passing over Rounded Profile	27
3.17	Validation of angular displacement and angular velocity while passing over Rounded Profile	28
3.18	Variation of daily equivalent static compression dose with velocity for driver	28
4.1	Multibody model of human body	30
4.2	Combined vehicle and human body model in ADAMS	31
4.3	Comparison of joint reaction forces on Elbow joint	33
4.4	Comparison of joint reaction forces on Shoulder joint	33
4.5	Comparison of joint reaction forces on Hip joint	33
4.6	Comparison of joint reaction forces on Knee joint	34
4.7	Comparison of joint reaction forces Head Neck Thorax joint	34

List of Tables

2.1	Dimensions of flat platform	11
2.2	Dimensions of Rounded Profile	11
3.1	Mass parameters of the bus	14
3.2	Suspension parameters of the bus	14
3.3	Geometry parameters of the bus	15
3.4	Mass parameters of the bus	24
3.5	Suspension parameters of the bus	24
3.6	Geometry parameters of the bus	25
4.1	Mass parameters of the human body	31
4.2	Torsional spring damper properties	31
4.3	Mass and Suspension parameters of the bus	32
4.4	Geometry parameters of the bus	32

Chapter 1

Introduction and Literature Review

1.1 Introduction

There are three major sources of vibration in vehicle this are the wheels, the driveline and the engine. The vibrations due to wheel of an on-road vehicle is pre dominantly excited by the unevenness of the road surface on which the vehicle travels. Road excitation reduces the ability of tires to exert forces in X and Y direction, because it causes a variable normal load F_z in Z direction, and increases the stressing of the structural elements. There various adverse effect of whole body vibration on human body like, vibrations with a frequency in the range between 0, 5 Hz and 80 Hz that may cause reduction of comfort, fatigue and health problems. Above 80 Hz the effect of vibration depends on the part of the body involved, as local vibration becomes the governing factor, making impossible to give general guide lines. There are resonance fields present, if any part of the body vibrates at particular resonance frequency which will cause serious damage of that body part.

1.2 Introduction to whole-body vibration

Whole-body vibration(WBV) is the vibration transmitted to person's entire body via his/her contact with a vibration source, usually through sitting or standing on a vibrating surface. WBV is common occupational problem for workers in high vibration environment, particularly when the exposure represents a significant part of their working day, not simply an intermittent event. Nowal days with high vibrating environment exposure to vibration is increased. In Europe, Canada and the U.S. about seven percent of the all workers regularly exposed to WBV. More than 400,000 cases of low back pain (LBP) in U.K. may be attributable to occupational WBV [1].

The effect of WBV on human body vary with various parameters like seating arrangement, seating position, posture and various physiological characteristics of exposed individuals. In standing posture compare to seated posture grater transmission of vertical vibration to lower spine. There are many biomechanic models has been developed to understand the biomechanics of WBV. As different human body part vibrates with different natural frequencis this frequency termed as resonant frequency(RF) so avoid exposure to vibration whose frequency matches with the resonant frequency(FR) of any

human body part.

Short-term or acute exposure to WBV results to physiological effect such as increase in heart rate, headache, motion sickness, muscle fatigue, discomfort and vision. Long-term exposure to WBV has adverse effect on human body, as repeated exposure may results in permanent psychological changes. Chronic exposure to WBV leads to degenerative disorders of the spine, especially the lumbar and thoracic spine and spinal disc disease and failure.

1.3 Literature review

In literature to study biodynamic of human body when exposed to WBV, number of mathematical models have been established. Human body is a very complex system whose mechanical properties vary from moment to moment and one individual to another. In past few decades no of mathematical models have been developed to investigate biodynamic response of human body under WBV. According to different modeling technique, these models can be grouped as multibody models, lumped-parameter models and finite element (FE) models.

Multibody model of human body consist of several rigid bodies interconnected by revolute joint in case of planar model and ball and socket in three-dimensional model. There are two types of multibody models, kinetic and kinematic models. The kinetic model concern with motion of each segment where as kinematic model deals with forces associated with motion. W. De Craecker developed two dimensional multibody model of human body model by spine modelling [2]. This model consist of rigid bodies which represent vertebrae and its surrounding, and spring-dampers, representing the dynamic behaviour of the intervertebral discs and the connecting ligaments. This spinal model consists of the sacrum (S), five lumbar vertebrae (L1-L5) and twelve thoracic vertebrae (T1-T12). Head and neck are modelled as a rigid structure, connected to the upper throacic vertebra(T1). Each vertebrae is connected to adjacent by a vertical translational pair of spring and damper, a horizontal translational pair of spring damper, and by a rotational pair of spring and damper. Another seven degree of freedom multibody model of human body is developed by Stefan Tabacu [3]. This model consider six major segments (pelvis, torso, head, hand, upper leg and lower leg) of human body and adjacent segments are connected by rotational spring.

Finite element (FE) model are complex and consists of numerous finite elements (FE) whose element properties were mainly obtained from experiments on human corpses. Today various powerful finite element (FE) analysis packages are available with the use of this packages we can easily analyse biodynamic response of human body. Accuracy of finite element (FE) model is depends on how accurate input human properties are used during simulation.

Lumped-parameter model consider the human body segment as point masses and this point masses are interconnected by spring and damper. This type of models are simple, computationally efficient and easy to validate with experiments. But disadvantage of this models is only one-directional analysis is possible. However to study effect of vertical vibration on driver and passenger this kind of models are very useful. There are thirteen lumped-parameter models has been developed , from one to eleven degrees of freedom(DOFs), and that includes linear and nonlinear models. Coermann's one-DOF model (Coermann, 1962) in this model seated body was constructed with single mass and connection between human body and seat is modeled by spring and damper, which represent physical properties of human body. A four-DOF human body model is proposed by Wael Abbas [5]. In this

model seated human body is constructed with four mass segments, this segments interconnected by five sets of spring damper. This four masses represents head and neck(m_1), torso(m_2), lower torso(m_3), and thigh and pelvis(m_4). This model used in half car model to predict the biodynamic response of seated human subjected to vertical vibrations due to road excitation.

A seven-DOF nonlinear lumped parameter model of seated human body is proposed by Patil and Palanichamy [6]. In this model human body consist of seven masses representing head and neck (m_1), back(m_2), upper torso(m_3), thorax(m_4), diaphragm(m_5), abdomen(m_6) and thighs and pelvis(m_7). The lumped masses are connected by spring and dashpot, representing the elastic and damping properties of connective tissue between segments.

Based on patil's seven-DOF model an eleven-DOF model is developed by Qassem and Othman [7]. The physical parameters mostly originated from Patil's model with nonlinearity of spring and damper neglected also back is further divided into cervical, thoracic and lumber spines. Compare to any other model this model give much more detail picture of human body. Apart from above mention human body models there are many other models also there, depending upon our requirement we can choose any of them.

1.4 Motivation, scope and objectives

People with long-term exposure to whole-body vibration (WBV), such as the occupational drivers, workers working in high vibrating environment, suffer health related consequences. Drivers short-term exposure to whole-body vibration causes muscle fatigue, ride discomfort and loss of balance, can affect the drivers ability to control the vehicle. To protect driver and passengers from health and safety risks caused by WBV, new methods should be implemented to reduce the exposure levels.

The main objective of this study is to reduce the WBV exposure levels by optimizing the passengers seat inclination and improving drivers grip over steering wheel while crossing speed hump.

No study was carried out to investigate the effect of seat inclination on the daily equivalent static compression dose. This investigation will be carried out at varying speeds while crossing different-different profiles of speed humps.

1.5 Thesis layout

This thesis consists of six chapters. Chapter 1 is the introduction of the research work with brief information about whole-body vibration. It also consist of literature review of human body model. A brief paragraph describes the motivation and scope.

Chapter 2: This chapter introduces ISO 2631-5:2004 standard. It talk about method of vibration measurement, daily equivalent static compression dose, assessment of adverse health effect of WBV on human body and speed hump.

Chapter 3: This chapter introduces 6 DOF and 5 DOF half car models, and various equations of motion for sprung and unsprung masses. The sprung mass equations of motion describe its longitudinal, transverse and pitch motion. Both models validated with ADAMS/View model and under

excitations due to speed hump S_{ed} calculated for both the models.

Chapter 4: This chapter covers different human body models, their mass distribution and various human body parameters. Human body model consist of six major boby parts namely: Head Neck, Thorax, upper leg, lower leg, arm and forearm. This human body model is combined with half car model and effect of tightly and loosely holding sreeging wheel on joint reaction forces is studied.

Chapter 5: This chapter summarizes the conclusion of all the research steps and the recommendations for the future work.

Chapter 2

Evaluation of Effect of Whole-Body Vibrations on Human Body

The International Organisation for Standardization(ISO) proposed several procedures to evaluate the effect of whole-body vibration(WBV) on human body. In ISO 2631-5:2004 standard [13], procedure to evaluate the effects of whole-body vibration on human body is proposed.

2.1 Evaluation according to ISO 2631-5:2004

ISO 2631-5:2004(E)

Mechanical vibration and shock - Evaluation of human exposure to whole-body vibration Part 5: Method for evaluation of vibration containing multiple shocks

This part of ISO 2631 deals with human exposure to mechanical multiple shocks measured at seat pad when a person is seated and does not voluntarily rise from the seat during exposure. The method described in this part of ISO 2631 is generally applicable in cases where adverse health effects in lumbar spine are concerned. It also gives detail procedure for the evaluation of vibrations effect to the human health. Based on the method described, the pressure exerted to the lumbar part of spinal column, consequent to shock vibrations, can be calculated. By comparison to the evaluation criteria, it is possible to assess the risk of getting health problems.

According to the procedure in ISO 2631-5:2004, the daily equivalent static compression dose (S_{ed}) is to be used for the evaluation effect of WBV on the human health. To calculate S_{ed} it requires acceleration response of the spine in all three translational direction. Predictive models are used to estimate the lumbar spine accelerations (a_{lx}, a_{ly}, a_{lz}) in the x-, y- and z-directions in response to accelerations measured at the seat pad (a_{sx}, a_{sy}, a_{sz}) along the same basicentric axes. In the x- and y-axes, the spinal response is approximately linear and is represented by a single-degree-of-freedom (SDOF) lumped-parameter model. In the z-direction, the spinal response is non-linear and is represented by a recurrent neural network model.

2.2 Calculation of acceleration dose and daily equivalent static compression dose

To calculate acceleration dose we need spinal response acceleration, spinal response acceleration is determined by using acceleration at seat pad. To get detail information about how to calculate spinal response acceleration from acceleration at seat pad please refer ISO 2631-5:2004(E) [13]. The acceleration dose, D_k , in meter per second square, in the k -direction is defined as:

$$D_k = \left[\sum_i A_{ik}^6 \right]^{1/6} \quad (2.1)$$

where:

A_{ik} is the i^{th} peak of the spine response acceleration $a_{ik}(t)$ and $k = x, y$ or z are directions of spine response acceleration.

A peak is defined as the maximum absolute value of the response acceleration between two consecutive zero crossing. Along x - and y -direction peaks in both positive and negative directions are counted. Along z -direction only peaks in the positive direction are counted. In equation 2.1 to calculate acceleration dose contribution of peaks of lower magnitude is not significant and therefore may be neglected. For assessment of health effect we need to calculate daily equivalent static compression dose for that we required average daily acceleration dose. The average daily acceleration dose, D_{kd} , in meters per second square is defined as

$$D_{kd} = D_k \left[\frac{t_d}{t_m} \right]^{1/6} \quad (2.2)$$

where:

t_d is the duration of daily exposure and t_m is the period over which D_k has been measured. Equation 2.2 is used when the total daily exposure is represented by a single measurement period. An equivalent static compressive stress, S_e , in megapascals, is calculated as follows:

$$S_e = \left[\sum_{k=x,y,z} (m_k D_k)^6 \right]^{1/6} \quad (2.3)$$

Where:

D_k is the acceleration dose in the k -direction. m_x , m_y and m_z are constants for x , y and z axis respectively. Recommended values for this constants are

$$m_x = 0.015 \text{ MPa}/(m/s^2)$$

$$m_y = 0.035 \text{ MPa}/(m/s^2)$$

$$m_z = 0.032 \text{ MPa}/(m/s^2)$$

The daily equivalent static compressive dose for lumbar spine that is parameter S_{ed} through the effect of shock vibration is evaluated, is obtained from equation 2.4 by normalising acceleration dose (D_k) to the average daily acceleration dose (D_{kd}). From the values of constants (m_x , m_y and m_z) it clear that weight given to acceleration along y -axis and z -axis is more than x -axis.

$$S_{ed} = \left[\sum_{k=x,y,z} (m_k D_{kd})^6 \right]^{1/6} \quad (2.4)$$

The procedure for calculation of the parameter S_{ed} and assessment of adverse health is described in the flow chart 2.1. The evaluation criteria for the parameter S_{ed} are set with the assumption that human body is exposed to shock vibrations during 240 days per year.

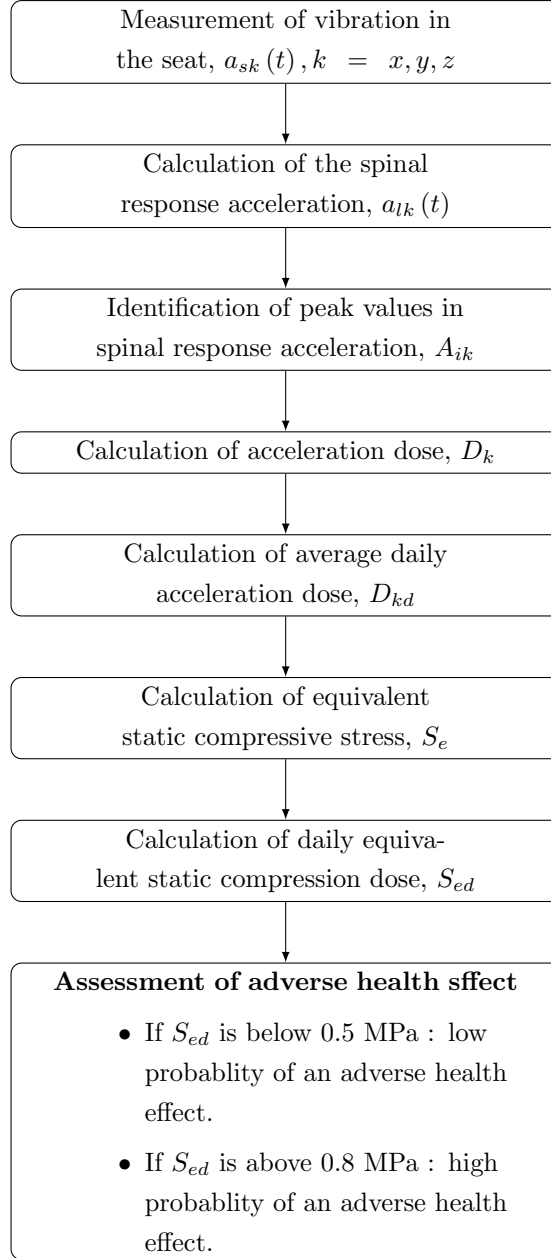


Figure 2.1: Flow chart for the assessment of adverse health effect

For the calculated values of the parameter S_{ed} one can estimate the effects of vibrations by comparing with the limit value - criteria as follows:

- If $S_{ed} < 0.5$ [MPa] the probability of negative effect of vibrations to health is low.
- If $S_{ed} > 0.8$ [MPa] the probability of negative effect of vibrations to health is significant.

If the S_{ed} is in between 0.5 MPa and 0.8 MPa the probability of negative effect of vibration is moderate.

Annex D of ISO 2631-5:2004 gives MATLAB program to calculate spinal response acceleration, a_{lk} , and acceleration dose, D_k from recorded acceleration time histories, a_{sk} , in the x-, y- and z-axis. As input data to this MATLAB program, an ASCII file with the extension .txt, and with two columns required, The first column contains the time data, and second column contain the measured acceleration in the seat, a_{sk} . By normalising acceleration dose to daily average acceleration dose, D_{kd} , daily equivalent static compression dose (S_{ed}) is calculated.

2.3 Speed Hump

A speed hump is a raised area in the roadway pavement surface extending across the travel way. Speed hump sometimes referred to as "pavement undulation" or "sleeping policeman". Speed humps are generally used for three purposes: (1) increasing the safety of residential streets, (2) improving the environmental quality of residential neighborhoods, and (3) improving traffic flow throughout a residential area, but in this study speed humps are used to induce excitations on front and rear axle of the vehicle. Speed "humps" are not the same as speed "bumps". The primary objective of these two devices is to control the speed of vehicles, but they have different designs and allowable uses. Speed hump profile is smooth, as compared to speed bump length of the speed hump is considerably large. Speed humps can also be installed in a series to reduce speeds along an extended section of street.

Speed bumps, on the other hand, have a more abrupt design. They consist of a portion of raised pavement and length of the raised pavement is considerably small, but because of their abruptness their use is very restricted. Speed bumps produce substantial driver discomfort, damage to the vehicle suspension, and/or loss of control if encountered at too high a speed. This is one reason speed bumps are not used on public roadways.

2.3.1 Classification of speed hump

Speed hump are classified based on the profile, height and length of speed hump. They are typically sinusoidal, circular, parabolic and flat-topped in shape and are a gentle version of the speed bump. For detail information on speed hump and its design refer [8]. Figure 2.2 shows a flat platform, and corresponding characteristic dimensions of flat platform are shown in Table 2.1.

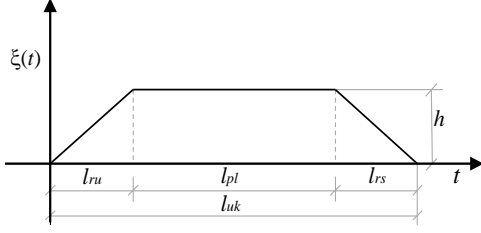


Figure 2.2: Flat platform

Geometry parameter		Value	
h	height of flat platform	0.08	m
l_{ru}	length of ascending ramp	1	m
l_{rs}	length of descending ramp	1	m
l_{pl}	length of flat platform	10	m
l_{uk}	overall length of flat platform	12	m

Table 2.1: Dimentions of flat platform

Figure 2.3 shows a rounded profile, and corresponding characteristic dimentions of rounded profile are shown in Table 2.2. Height and length of flat platform is more than rounded profile.

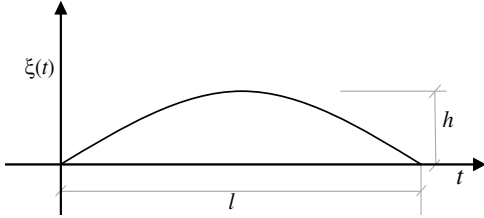


Figure 2.3: Rounded Profile

Geometry parameter		Value	
h	height of flat platform	0.05	m
l	length of profile	0.96	m

Table 2.2: Dimentions of Rounded Profile

The analytic expression describing speed hump in the form of flat platform is given by equation 2.5, and one describing rounded profile speed hump is given by equation 2.6.

$$\xi(t) = \left\{ \begin{array}{l} \frac{h}{l_{ru}} \cdot V \cdot t \quad , 0 \leq t < \frac{l_{ru}}{V} \\ h \quad , \frac{l_{ru}}{V} \leq t \leq \frac{l_{ru} + l_{pl}}{V} \\ -\frac{h}{l_{rs}} \cdot V \cdot t + \frac{h \cdot (l_{ru} + l_{pl})}{l_{rs}} + h \quad , \frac{(l_{ru} + l_{pl})}{V} < t \leq \frac{(l_{ru} + l_{pl} + l_{rs})}{V} \\ 0 \quad , t > \frac{(l_{ru} + l_{pl} + l_{rs})}{V} \end{array} \right\} \quad (2.5)$$

$$\xi(t) = \left\{ \begin{array}{l} h \cdot \sin\left(\frac{\pi \cdot V}{l}\right) \quad , 0 \leq t \leq \frac{l}{V} \\ 0 \quad , t > \frac{l}{V} \end{array} \right\} \quad (2.6)$$

where, V is the velocity of car.

To give excitation on front and rear axle, this two profiles of speed hump are used, when car passes over the speed hump it excites front and rear axle.

2.4 Summary

This chapter has dealt with ISO 2631-5:2004 standard and speed humps. ISO 2631-5:2004 deals with human exposure to mechanical multiple shocks measured at seat pad when a person is seated. The method described in ISO 2631-5:2004 is generally applicable in cases where adverse health effects in lumbar spine are concerned. According to the procedure in ISO 2631-5:2004, the daily equivalent static compression dose, S_{ed} is to be used for the evaluation adverse effect of WBV on human health. If $S_{ed} < 0.5$ [MPa] the probability of negative effect of vibrations to health is low. If $S_{ed} > 0.8$ [MPa] the probability of negative effect of vibrations to health is significant.

A speed hump is a raised area in the roadway pavement surface extending across the travel way. In this study speed humps are used to induce excitations on front and rear axle of the vehicle. Speed humps are not same as speed bumps. Profile of the speed hump is smooth on the other hand speed bumps has more abrupt design so speed bump produce substantial driver discomfort. Speed humps are classified based on the profile, height and length of hump.

Chapter 3

Half Car Models and Analysis

3.1 6 DOF Half car model introduction

The schematic diagram 3.1 shows the planr half car with two rigid axles and pneumatic suspension system. Where m is the mass of car (Sprung Mass), J_y is the mass moment of inertia of the car about (transversal) y -axis, m_{t1} and m_{t2} are the masses of front axle (front unsprung mass) and rear axle (rear unsprung mass) respectively. Spring damper attached between sprung mass and unsprung mass represents suspension system of the vehicle. To represent passengers we use single-degree-of-freedom lumped-parameter model, where m_{p1} and m_{p2} are masses of passenger1 and passenger2 respectively. c_{p1} and b_{p1} is the passenger1's seat spring stiffness and damping, similarly c_{p2} and b_{p2} is the passenger2's seat spring stiffness and damping. Sprung mass has two degrees of freedom which are vertical displacement (bounce, z) at the center of gravity and angular motion (pitching, θ) of the sprung mass around the (transversal) y -axis. Vertical displacement of front axle (z_{t1}), rear axle (z_{t2}), passenger1 (z_{p1}) and pasenger2 (z_{p2}) represents another four degrees of freedom. In all this half car model has six degrees of freedom. For detail information about six degrees of freedom half car model refer [4].

This half car model has been defined according to the following assumptions:

- The car is symmetrical about longitudinal (x) axis.
- There is no angular movement around x -axis.
- The excitations on both front and rear axle are the same.
- All possible displacements of concentrated masses around the static equilibrium position are small.
- All elastic and damping characteristic of suspension system are linear.
- There is always contact between tire and ground.
- The car movement is linear and at constant speed.

In this model, the disturbances ξ_1 and ξ_2 are caused by speed hump at front and rear axle when vchile is passing over the speed hump. This model is used to investigate the biodynamic response of vehicles under random road input excitations.

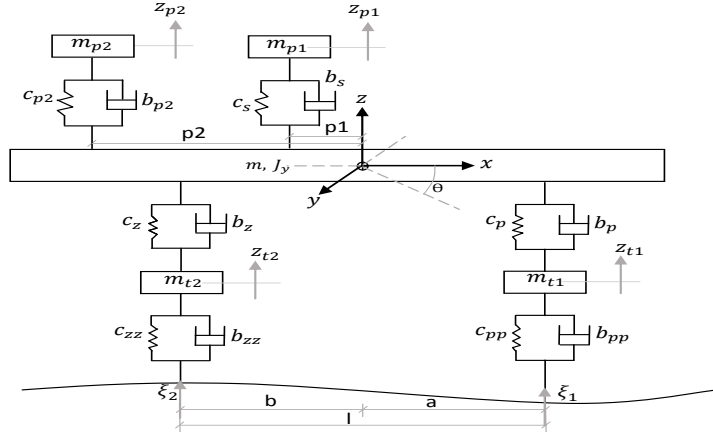


Figure 3.1: 6 DOF Half Car Model

3.1.1 6 DOF half car model parameters

The meaning of the parameters in figure 3.1 and corresponding values shown in Tables 3.1, 3.2 and 3.3. The values are assumed after the relevant literature (Nijemčević, et al., 2001; Mladenović, 1997; Simić, 1979) [4].

Mass parameter		Value	
m_{p1}	mass of the passenger1	80	kg
m_{p2}	mass of the passenger2	80	kg
m	suspended mass of the partially loaded bus	11900	kg
m_{t1}	mass of the front axle	745	kg
m_{pt2}	mass of the rear axle	1355	kg
J_y	inertia moment of the suspended mass related to transversal axis	50000	kgm^2

Table 3.1: Mass parameters of the bus

Suspension parameter		Value	
c_{p1}, c_{p2}	passengers seat spring stiffness	950000	N/m
b_{p1}, b_{p2}	passengers seat damping	200	Ns/m
c_p	stiffness of front axle suspension element	350000	N/m
b_p	front axle shock absorbers damping	800000	Ns/m
c_z	stiffness of rear axle suspension element	811250	N/m
b_z	damping for rear axle absorbers	91265	Ns/m
c_{pp}	front axle tire stiffness	2000000	N/m
b_{pp}	front axle tire damping	300	Ns/m
c_{zz}	rear axle tire stiffness	4000000	N/m
b_{zz}	rear axle tire damping	600	Ns/m

Table 3.2: Suspension parameters of the bus

Geometry parameter		Value	
l	distance between axles	5.65	m
a	distance from the front axle to CG	3.12	m
b	distance from the rear axle to CG	2.53	m
P_1	distance from passenger1's seat to CG	-0.10	m
P_2	distance from the passenger2's seat to CG	-4.23	m

Table 3.3: Geometry parameters of the bus

3.1.2 Equations of motion for 6 DOF half car model

For small and linear vibrations we can use Lagrange equations to derive equation's of motion, so general Lagrange equation is written as:

$$\frac{d}{dt} \left(\frac{\partial L}{\partial \dot{q}_i} \right) - \frac{\partial L}{\partial q_i} + \frac{\partial P}{\partial \dot{q}_i} = 0 \quad (3.1)$$

where, \dot{q}_i and q_i are independent variables and L is Lagrangian function, which is defined as the difference between kinetic and potential energies of the dynamic system. P is the dissipation function of the system.

To study the effect of shock vibrations on passenger's health, the differential equations of motion for concentrated masses of half car model are required. Using the lagrange's equation, and considering earlier assumptions, the differential equations of motion for the above half car model are defined by following equations (Eq. (3.2) - Eq. (3.7)) [4].

$$m_{p1}\ddot{z}_{p1} + b_{p1}\dot{z}_{p1} + c_{p1}z_{p1} - b_{p1}\dot{z} - c_{p1}z + b_{p1}P_1\dot{\theta} + c_{p1}P_1\theta = 0 \quad (3.2)$$

$$m_{p2}\ddot{z}_{p2} + b_{p2}\dot{z}_{p2} + c_{p2}z_{p2} - b_{p2}\dot{z} - c_{p2}z + b_{p2}P_2\dot{\theta} + c_{p2}P_2\theta = 0 \quad (3.3)$$

$$\begin{aligned} m\ddot{z} + (b_{p1} + b_{p2} + b_p + b_z)\dot{z} + (c_{p1} + c_{p2} + c_p + c_z)z + (ab_p - P_1b_{p1} - P_2b_{p2} - bb_z)\dot{\theta} \\ + (ac_p - P_1c_{p1} - P_2c_{p2} - bc_z)\theta - b_{p1}\dot{z}_{p1} - c_{p1}z_{p1} - b_{p2}\dot{z}_{p2} - c_{p2}z_{p2} - b_p\dot{z}_{t1} - c_pz_{t1} \\ - b_z\dot{z}_{t2} - c_zz_{t2} = 0 \end{aligned} \quad (3.4)$$

$$\begin{aligned} J_y\ddot{\theta} + (P_1^2b_{p1} + P_2^2b_{p2} + a^2b_p + b^2b_z)\dot{\theta} + (P_1^2c_{p1} + P_2^2c_{p2} + a^2c_p + b^2c_z)\theta \\ + (ab_p - P_1b_{p1} - P_2b_{p2} - bb_z)\dot{z} + (ac_p - P_1c_{p1} - P_2c_{p2} - bc_z)z + P_1b_{p1}\dot{z}_{p1} \\ + P_1c_{p1}z_{p1} + P_2b_{p2}\dot{z}_{p2} + P_2c_{p2}z_{p2} - ab_p\dot{z}_{t1} - ac_pz_{t1} + bb_z\dot{z}_{t2} + bc_zz_{t2} = 0 \end{aligned} \quad (3.5)$$

$$m_{t1}\ddot{z}_{t1} + (b_p + b_{pp})\dot{z}_{t1} + (c_p + c_{pp})z_{t1} - b_p\dot{z} - c_pz - ab_p\dot{\theta} - ac_p\theta = b_{pp}\dot{\xi}_1 + c_{pp}\xi_1 \quad (3.6)$$

$$m_{t2}\ddot{z}_{t2} + (b_z + b_{zz})\dot{z}_{t2} + (c_z + c_{zz})z_{t2} - b_z\dot{z} - c_zz - bb_z\dot{\theta} - bc_z\theta = b_{zz}\dot{\xi}_2 + c_{zz}\xi_2 \quad (3.7)$$

3.2 6 DOF half car model in ADAMS/View

Figure 3.2 shows 6 DOF half car model in ADAMS/View. In this model passenger1, passenger2, bus, front axle and rear axle are represented by different parts. This parts are inter connected by using thanslational spring damper which acts like suspension. At the C.G. of each box planar and translational joint is added. Planar joint allows motiom of this parts in a plane only. Translational joint at the C.G of passenger acts like seat belt and allows linear motion along the direction of translational joint. This ADAMS/View model and above mention 6 DOF half car model has identical dimentions, mass, stiffness and damping properties. To give excitations due to speed hump on front and rear axle motion command is used in ADAMS/View. All the assumptions made in 6 DOF half car model are also applicable for this model.

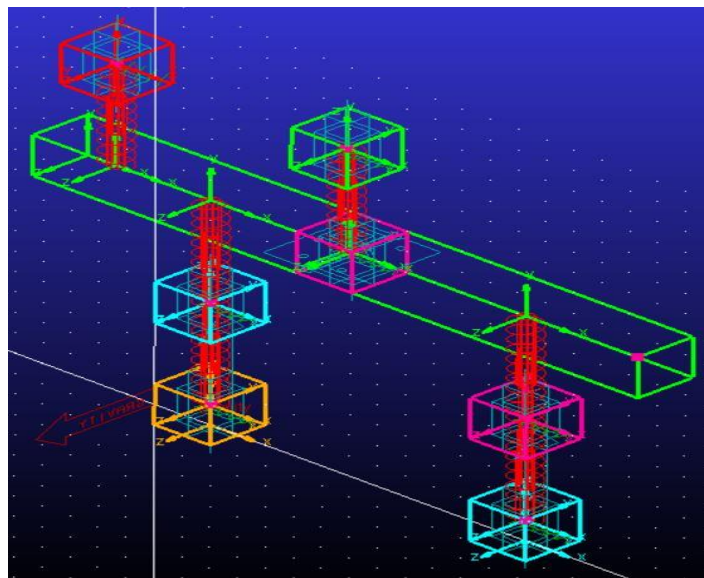
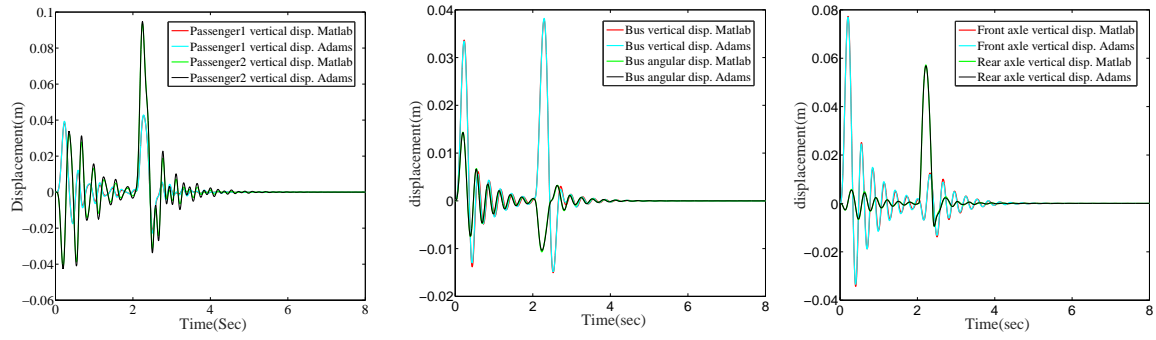


Figure 3.2: 6 DOF Half Car Model in ADAMS/View

3.3 Validation of 6 DOF model with ADAMS

To validate 6 DOF half car model with ADAMS/View, numerical solving of the differential equations of motion of 6 DOF half car model is done through the program written in MATLAB and MATLAB's 'ode45' function is used for that. To simulate half car model in ADAMS/View GSTIFF solver is used. Excitation on front and rear axle in both the models are same and is described by rounded profile speed hump. The time of simulation is limited to 8 seconds for both the MATLAB and ADAMS/View simulation.

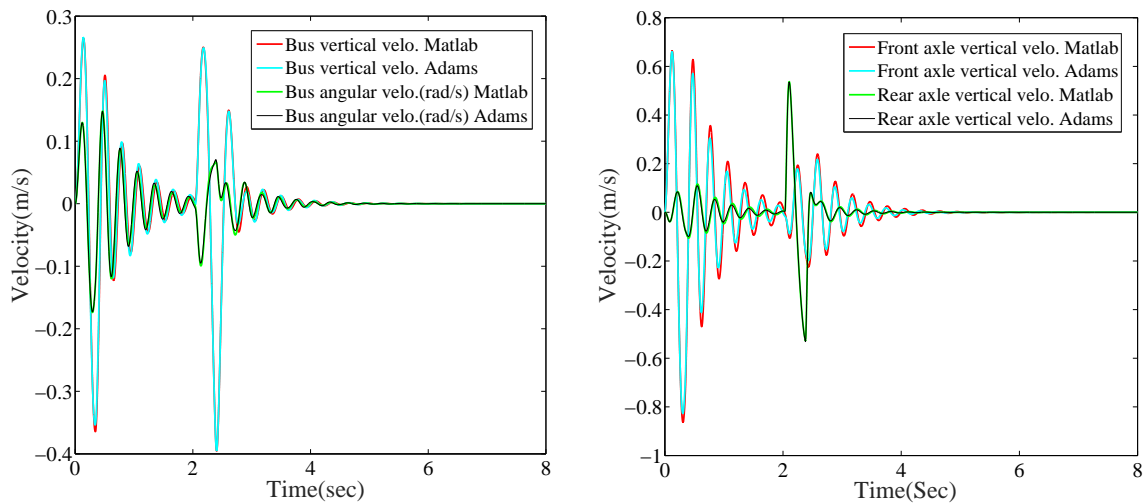
All validation's are carried out by giving constant velocity 10 km/h to the vehicle.



(a) Displacement(m) Vs Time(Sec) (b) Displacement(m) Vs Time(Sec) (c) Displacement(m) Vs Time(Sec)

Figure 3.3: Validation of displacement while passing over Rounded Profile

Figure 3.3 and figure 3.4 shows comparison of displacement and velocity for passeger1, passengr2, bus, front axle and rear axle. From figure 3.3 and figure 3.4, it is clear that displacement and velocity of both MATLAB and ADAMS/View model almost matching.



(a) Velocity(m/s) Vs Time(Sec) (b) Velocity(m/s) Vs Time(Sec)

Figure 3.4: Validation of velocity while passing over Rounded Profile

3.4 Daily equivalent static compression dose

ADAMS/View model is simulated at various speeds ranging from 10 km/h to 50 km/h and at each speed seat acceleration for pasenger1 and passenger2 is recorded. As this is planr model and their is no acceleration along longitudinal (x-axis) and transversal (y-axis) directions, only the vertical acceleration (along z-axis) on the passsenger1 and passenger2 is recorded. This numerical data is exported from ADAMS/View post processor and saved in ASCII file with the extension .txt, and with two columns. The first column contains time data, and second column contain

measured acceleration in the seat. After recording passenger's seat acceleration this data is given as input to the MATLAB program in Annex D of ISO 2631-5:2004. This MATLAB program gives Daily average acceleration, D_{kd} as output. Using equation 2.4 daily equivalent static compression dose(S_{ed}) is calculated.

The analysis is made for two positions of sitting passenger, one in the middle part of the bus (passenger1) and another on the rear end (overhang) of the bus (passenger2).

Figure 3.5 shows in both cases, the parameter S_{ed} has highest value for the passenger2. In case of flat platform, values of parameter S_{ed} for passenger2 crosses both criteria 0.5 MPa and 0.8 MPa, when bus speed is grater than 18 km/h and 21 km/h respectively. For the bus speed of 50 km/h the value of parameter S_{ed} is highest, so at this speed shock vibrations has high negative effect to his health. For the passenger1 value of parameter S_{ed} are lower than 0.5 MPa for all bus speeds, so the risk of negative infulance of shock vibrations on the health of passenger1 is low (figure 3.5 (b)).

While passing over speed hump with rounded profile, passenger2 crosses both the criteria when speed is above 12 km/h. Passenger1 crosses criteria of 0.5 MPa, at bus speed grater than 36 km/h (figure 3.5 (a)).

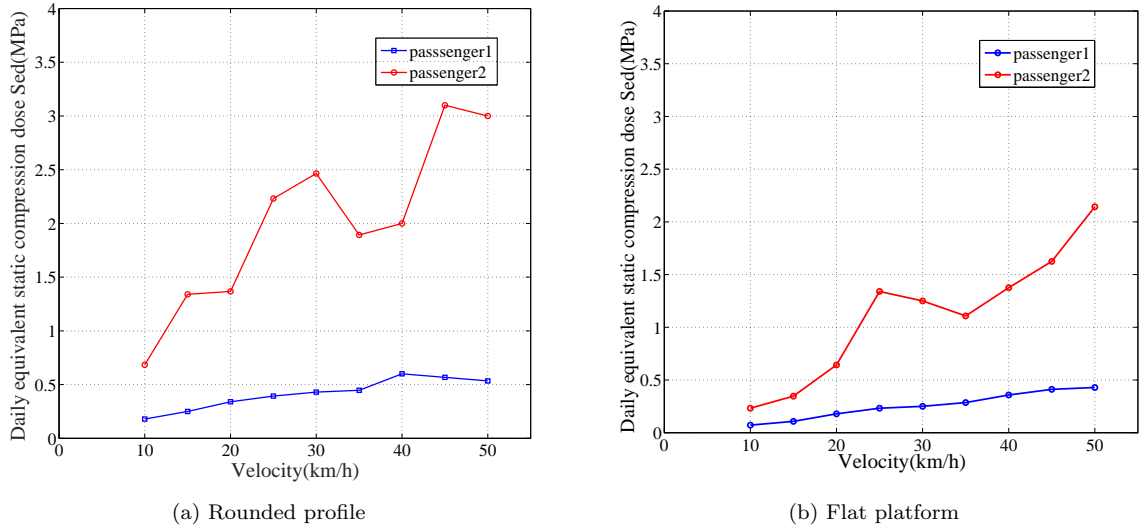


Figure 3.5: Variation of daily equivalent static compression dose with velocity

3.5 Inclined 6 DOF half car model

According to ISO 2631-5:2004 different postures can result in different responses in the spine. To investigate the effect of seat inclination on human body, a inclined 6 DOF half car model is build in ADAMS/View. In this model both the passenger's inclined with vertical axis. To represent seat inclination at C.G. of each passenger one translational joint is added. A translational joint allows one part to translate along a vector with respect to a another part. The parts can only translate, no rotation is possible with resepect to another part. Translational joint acts as a seat belt in real vehicle. The orientation of the translational joint, determines the direction of the axis along which parts can slide with respect to each other. By changing the direction of orientation vector seat is

inclined with respect to vertical direction.

Figure 3.6 shows inclined 6 DOF half car model in ADAMS/View. In this model passenger1, passenger2, are inclined with respect to vertical direction (z-axis). This ADAMS/View model and above mention 6 DOF half car model has identical dimentions, mass, stiffness and damping properties. Only difference is orientation of passengers, in this model passengers are inclined with vertical direction. To give excitations due to speed hump on front and rear axle adams motion command is used. Excitation on front and rear axle in both the models are same and is described by rounded profile speed hump. All the assumptions made in 6 DOF half car model are also applicable to this model

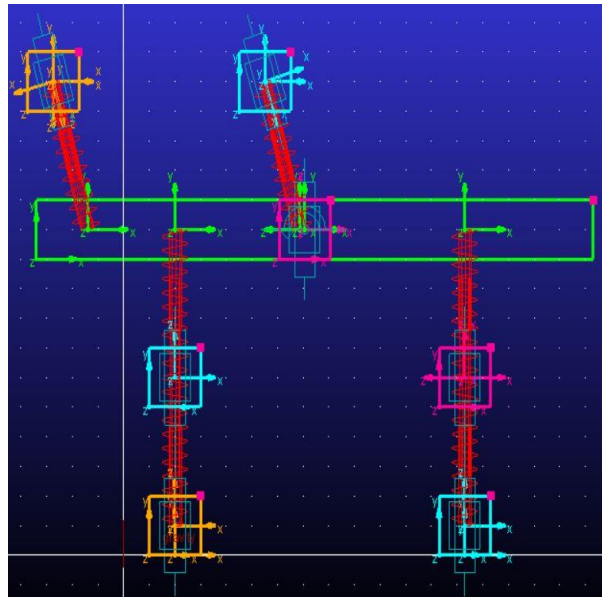


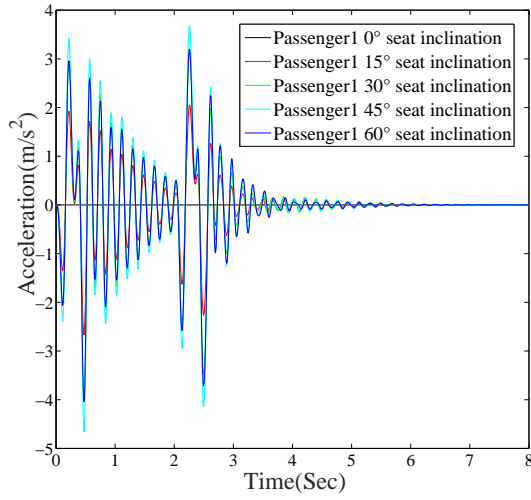
Figure 3.6: Inclined 6 DOF Half Car Model in ADAMS/View

3.5.1 Effect of seat inclination on acceleration

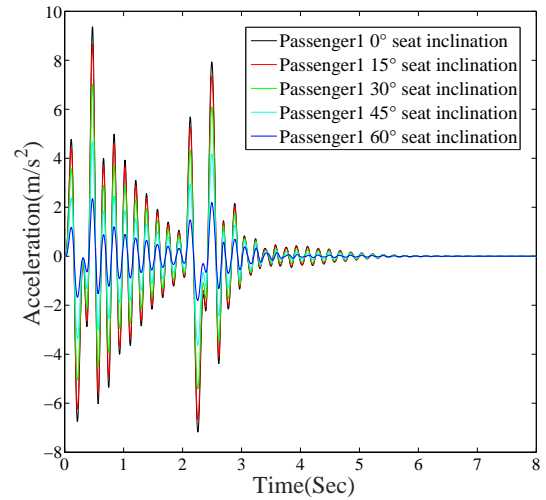
To investigate effect of seat inclination on health of passenger, passenger's seat is inclined with respect to vertical by 15° , 30° , 45° and 60° . For each seat inclination model is simulated in ADAMS/Views for 8 seconds. Excitation on front and rear axle for this simulation is described by rounded profile speed hump.

All the simulations are carried out by giving constant velocity 10 km/h to the vehicle. Compared to previous model here seats are inclined, because of seat inclination each passenger will have two components of acceleration. One component along longitudinal (x-axis) and another along transverse (z-axis) direction.

Figure 3.7 shows effect of seat inclination on acceleration of passenger1 along x-axis and y-axis. For passenger1 as the seat inclination increase from 0° to 60° acceleration along x-axis increase gradually but at the same time acceleration along z-axis decrease drastically. Similarly figure 3.8 shows effect of seat inclination on acceleration of passenger2. With seat inclination acceleration along x-axis increases and acceleration along z-axis decreases.

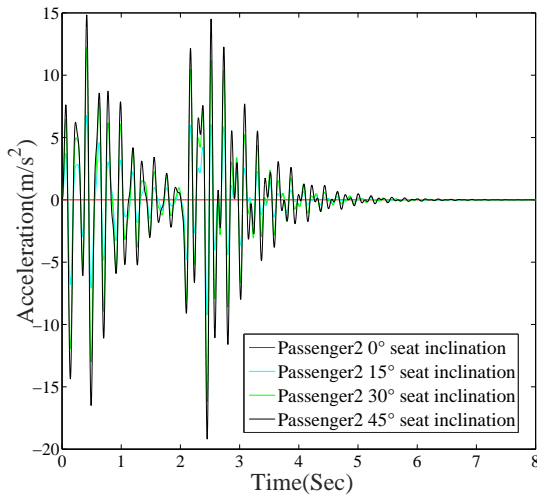


(a) Passenger1 Acceleration (m/s^2) Vs Time(Sec) along x-axis

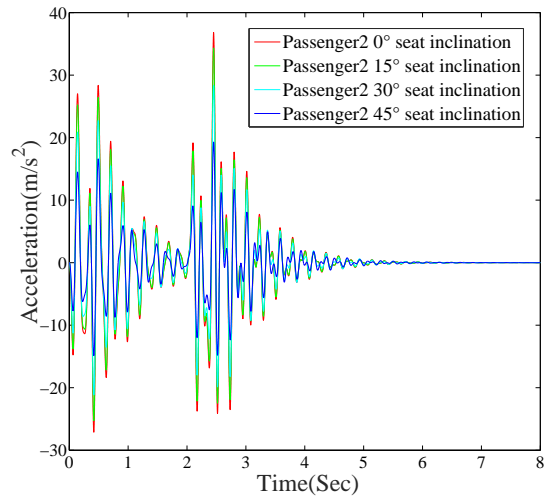


(b) Passenger1 Acceleration (m/s^2) Vs Time(Sec) along z-axis

Figure 3.7: Effect of seat inclination on acceleration of passenger1



(a) Passenger2 Acceleration (m/s^2) Vs Time(Sec) along x-axis



(b) Passenger2 Acceleration (m/s^2) Vs Time(Sec) along z-axis

Figure 3.8: Effect of seat inclination on acceleration of passenger2

From figure 3.7 and figure 3.8 it clear that while crossing speed hump passenger2 experiences more acceleration than passenger1. This is because passenger1 is seated in the middle of the bus and passenger2 is seated in the rear end of the bus. As passenger2 experiencing more acceleration, he will face more discomfort. Effect of shock vibration on the health of rear seated passenger is adverse.

3.5.2 Effect of seat inclination on daily equivalent static compression dose

To study effect of seat inclination on daily equivalent static compression dose for passenger1 and passenger2, five models with seat inclination 0° , 15° , 30° , 45° and 60° are build in ADAMS/View. The excitations due to flat platform and rounded profile is given as input to front and rear axle. This ADAMS/View model under excitatons dut to flat platform and rounded profile, simulated at various speeds ranging from 10 km/h to 50 km/h. For each model at all speeds seat acceleration for passenger1 and passenger2 is recorded and saved with .txt extension. As seat is inclined both the passenger has two components of acceleration, one along x-axis and another along z-axis. Using annex D of ISO 2631-5:2004 daily equivalent static compression dose is calculated.

Figure 3.9 shows variation of S_{ed} with seat inclination and speed for passenger1 while crossing rounded profile speed hump. With increasing seat inclination at all speeds, S_{ed} along x-axis increases (figure 3.9 (a)). S_{ed} along z-axis with increasing seat inclination decreases significantly (figure 3.9 (b)). Assessment of adverse health effect is based on overall (cosidering acceleration along x-, y- and z-axis) acceleration. To calculate overall S_{ed} , considering acceleration along both the axis equation 2.4 is used. In equation 2.4 compared to y-axis ($m_y = 0.035 \text{ MPa}/(m/s^2)$) and z-axis ($m_z = 0.032 \text{ MPa}/(m/s^2)$) weight given to x-axis ($m_x = 0.015 \text{ MPa}/(m/s^2)$) accelearton is very small. So the effect of acceleration along x-axis on overall S_{ed} is negligible. Figure 3.9 (c) shows overall S_{ed} for passenger1 while crossing rounded profile speed hump, which is almost same as figure 3.9 (b).

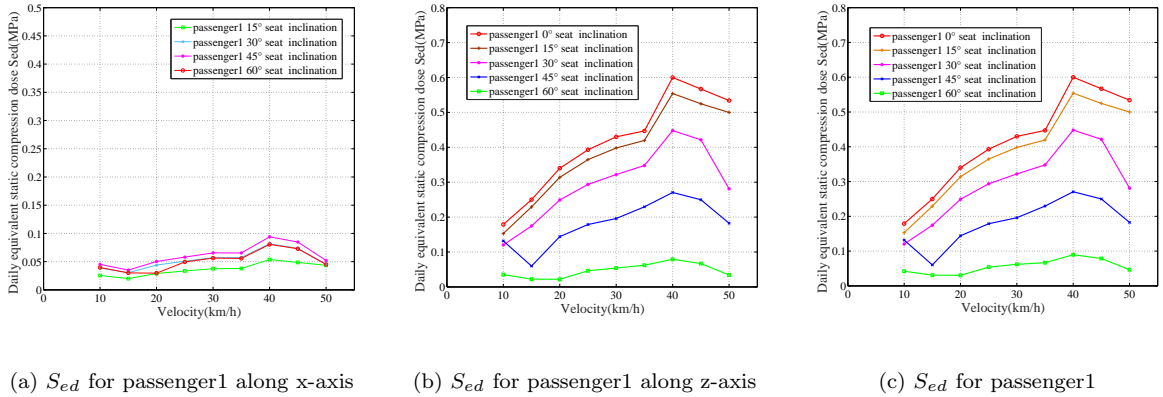


Figure 3.9: Variation of daily equivalent static compression dose with velocity over rounded profile

Figure 3.10 shows variation of S_{ed} with seat inclination and speed for passenger1 while crossing flat platform speed hump. With increasing seat inclination at all speeds, S_{ed} along x-axis increases (figure 3.10 (a)). S_{ed} along z-axis with increasing seat inclination decreases significantly (figure 3.10 (b)). Overall S_{ed} for passenger1 while crossing flat platform speed hump decreases with increasing seat inclination (figure 3.10 (c)).

For passenger1 with increasing seat inclination and while crossing both speed hump's S_{ed} decreases significantly. At 60° seat inclination S_{ed} decreases below 0.1 MPa fro all speeds. The probability of negative effect of vibrations to health is very low at 60° seat inclination.

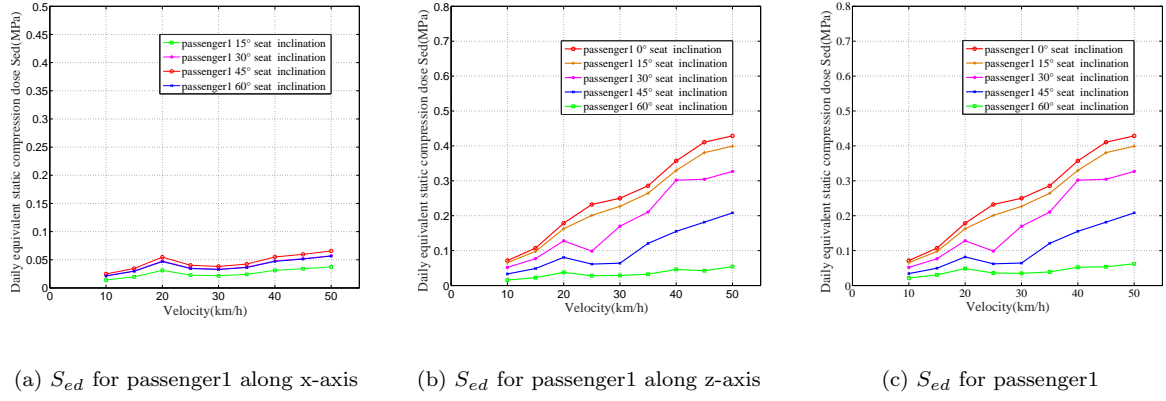


Figure 3.10: Variation of daily equivalent static compression dose with velocity over flat platform

Figure 3.11 shows variation of S_{ed} with seat inclination and speed for passenger2 while crossing rounded profile speed hump. With increasing seat inclination at all speeds, S_{ed} along x-axis increases (figure 3.11 (a)). S_{ed} along z-axis with increasing seat inclination decreases significantly (figure 3.11 (b)). Overall S_{ed} for passenger2 while crossing rounded profile speed hump decreases with increasing seat inclination (figure 3.11 (c)). Passenger2 is rear seated and experiences more acceleration, when speed is above 22 km/h at 60° seat inclination S_{ed} crosses both the criteria. The probability of negative effect of vibrations to health is still high at 60° seat inclination.

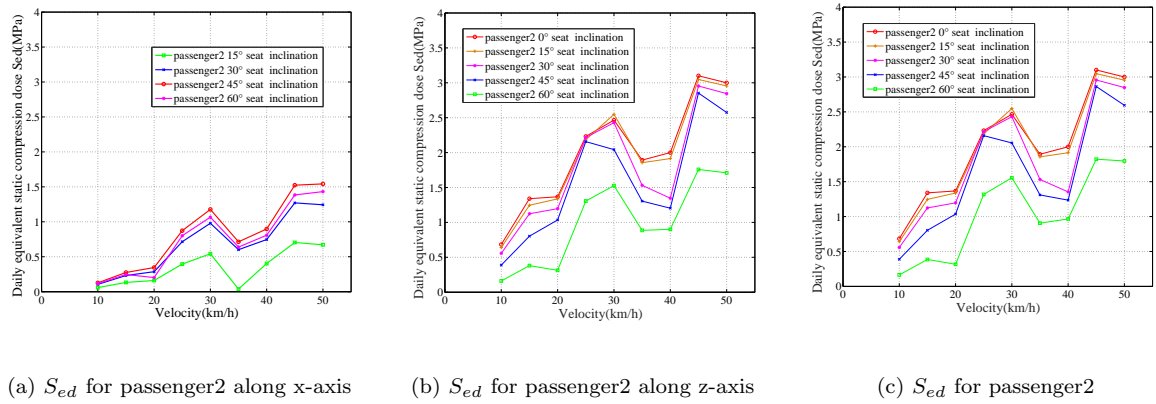


Figure 3.11: Variation of daily equivalent static compression dose with velocity over rounded profile

Figure 3.12 shows variation of S_{ed} with seat inclination and speed for passenger2 while crossing flat platform speed hump. With increasing seat inclination at all speeds, S_{ed} along x-axis increases (figure 3.12 (a)). S_{ed} along z-axis with increasing seat inclination decreases significantly (figure 3.12 (b)). Overall S_{ed} for passenger1 while crossing flat platform speed hump decreases with increasing seat inclination (figure 3.12 (c)). For passenger2 when speed is below 42 km/h and 60° seat inclination S_{ed} is below 0.5 MPa. The probability of negative effect of vibrations on health is low at 60° seat inclination.

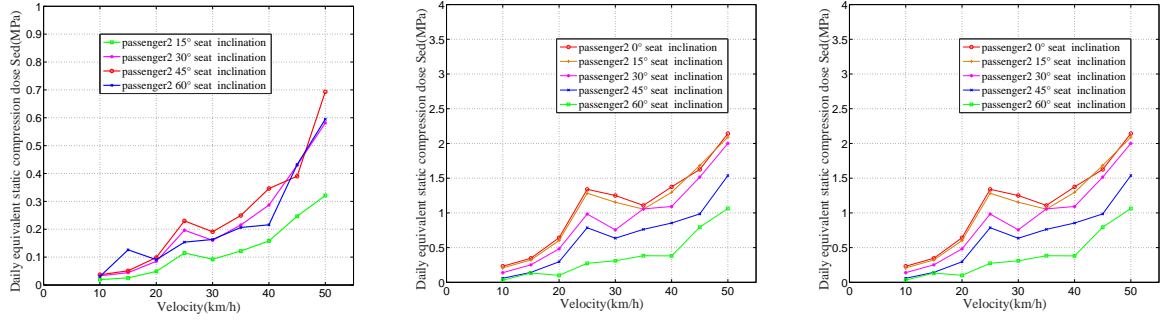
(a) S_{ed} for passenger2 along x-axis(b) S_{ed} for passenger2 along z-axis(c) S_{ed} for passenger2

Figure 3.12: Variation of daily equivalent static compression dose with velocity over flat platform

3.6 5 DOF Half car model introduction

The schematic diagram 3.13 shows the planar half car with two rigid axles and pneumatic suspension system. Where m is the mass of car (Sprung Mass), J_y is the mass moment of inertia of the car about (transversal) y-axis, m_{t1} and m_{t2} are the masses of front axle (front unsprung mass) and rear axle (rear unsprung mass) respectively. Spring damper attached between sprung mass and unsprung mass represents suspension system of the vehicle. To represent driver we use single-degree-of-freedom lumped-parameter model, where m_s is the mass of driver. c_s and b_s is the driver's seat spring stiffness and damping. Sprung mass has two degrees of freedom which are vertical displacement (bounce, z) at the center of gravity and angular motion (pitching, θ) of the sprung mass around the (transversal) y-axis. Vertical displacement of front axle (z_{t1}), rear axle (z_{t2}) and driver (z_s) represents another three degrees of freedom. In all this half car model has five degrees of freedom. For detail information about five degree's of freedom half car model refer [9].

This half car model has been defined according to the following assumptions:

- The car is symmetrical about longitudinal (x) axis.
- There is no angular movement around x -axis.
- The excitations on both front and rear axle are the same.
- All possible displacements of concentrated masses around the static equilibrium position are small.
- All elastic and damping characteristic of suspension system are linear.
- There is always contact between tire and ground.
- The car movement is linear and at constant speed.

In this model, the disturbances ξ_1 and ξ_2 are caused by speed hump at front and rear axle when vehicle passing over the speed hump. This model is used to investigate the biodynamic response of vehicles under random road input excitations.

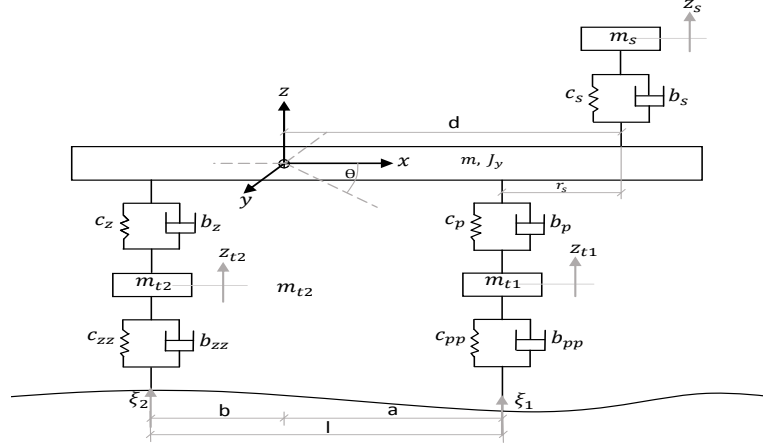


Figure 3.13: 5 DOF Half Car Model

3.6.1 5 DOF half car model parameters

The meaning of the parameters in figure 3.13 and corresponding values shown in Tables 3.4, 3.5 and 3.6. The values are assumed after the relevant literature (Nijemčević, et al., 2001; Mladenović, 1997; Simić, 1979) [9].

Mass parameter		Value	
m_s	mass of the driver and the seat	100	kg
m	suspended mass of the partially loaded bus	11900	kg
m_{t1}	mass of the front axle	745	kg
m_{pt2}	mass of the rear axle	1355	kg
J_y	inertia moment of the suspended mass related to transversal axis	50000	kgm^2

Table 3.4: Mass parameters of the bus

Suspension parameter		Value	
c_s	driver's seat spring stiffness	8500	N/m
b_s	driver's seat damping	650	Ns/m
c_p	stiffness of front axle suspension element	350000	N/m
b_p	front axle shock absorbers damping	800000	Ns/m
c_z	stiffness of rear axle suspension element	811250	N/m
b_z	damping for rear axle absorbers	91265	Ns/m
c_{pp}	front axle tire stiffness	2000000	N/m
b_{pp}	front axle tire damping	300	Ns/m
c_{zz}	rear axle tire stiffness	4000000	N/m
b_{zz}	rear axle tire damping	600	Ns/m

Table 3.5: Suspension parameters of the bus

Geometry parameter		Value	
l	distance between axles	5.65	m
a	distance from the front axle to CG	3.12	m
b	distance from the rear axle to CG	2.53	m
r_s	distance from the driver's seat to the front axle	1.50	m
d	diatance from the driver's seat to CG	-4.23	m

Table 3.6: Geometry parameters of the bus

3.6.2 Equations of motion for 5 DOF half car model

For small and linear vibrations we can use Lagrange equations to derive equations of motion, so general Lagrange equation is written as

$$\frac{d}{dt} \left(\frac{\partial L}{\partial \dot{q}_i} \right) - \frac{\partial L}{\partial q_i} + \frac{\partial P}{\partial \dot{q}_i} = 0 \quad (3.8)$$

where, \dot{q}_i and q_i are independent variables and L is Lagrangian function, which is defined as the difference between kinetic and potential energies of the dynamic system. P is the dissipation function of the system.

To study the effect of shock vibrations on passenger's health, the differential equations of motion for concentrated masses of half car model are required. Using the lagrange's equation, and considering earlier assumptions, the differential equations of motion for the above half car model are defined by following equations (Eq. (3.9) - Eq. (3.13)) [9].

$$m_s \ddot{z}_s + b_s \dot{z}_s + c_s z_s - b_s \dot{z} - c_s z - b_s d \dot{\theta} + c_s d \theta = 0 \quad (3.9)$$

$$m \ddot{z} + (b_s + b_p + b_z) \dot{z} + (c_s + c_p + c_z) z + (db_s + ab_p - bb_z) \dot{\theta} + (dc_s + ac_p - bc_z) \theta - b_s \dot{z}_s - c_s z_s - b_p \dot{z}_{t1} - c_p z_{t1} - b_z \dot{z}_{t2} - c_z z_{t2} = 0 \quad (3.10)$$

$$J_y \ddot{\theta} + (P_1^2 b_{p1} + P_2^2 b_{p2} + a^2 b_p + b^2 b_z) \dot{\theta} + (P_1^2 c_{p1} + P_2^2 c_{p2} + a^2 c_p + b^2 c_z) \theta + (ab_p - P_1 b_{p1} - P_2 b_{p2} - bb_z) \dot{z} + (ac_p - P_1 c_{p1} - P_2 c_{p2} - bc_z) z + P_1 b_{p1} \dot{z}_{p1} + P_1 c_{p1} z_{p1} + P_2 b_{p2} \dot{z}_{p2} + P_2 c_{p2} z_{p2} - ab_p \dot{z}_{t1} - ac_p z_{t1} + bb_z \dot{z}_{t2} + bc_z z_{t2} = 0 \quad (3.11)$$

$$m_{t1} \ddot{z}_{t1} + (b_p + b_{pp}) \dot{z}_{t1} + (c_p + c_{pp}) z_{t1} - b_p \dot{z} - c_p z - ab_p \dot{\theta} - ac_p \theta = b_{pp} \dot{\xi}_1 + c_{pp} \xi_1 \quad (3.12)$$

$$m_{t2} \ddot{z}_{t2} + (b_z + b_{zz}) \dot{z}_{t2} + (c_z + c_{zz}) z_{t2} - b_z \dot{z} - c_z z - bb_z \dot{\theta} - bc_z \theta = b_{zz} \dot{\xi}_2 + c_{zz} \xi_2 \quad (3.13)$$

3.7 5 DOF Half car model in ADAMS/View

Figure 3.14 shows 5 DOF half car model in ADAMS/View. In this model driver, bus, front axle and rear axle are represented by different parts. This parts are inter connected by using thanslational spring damper which acts like suspension. At the C.G. of each part planar and translational joint

is added. planar joint allows motion of these parts in a plane only. Translational joint at the C.G of passenger acts like seat belt and allows linear motion along the direction of translational joint. This ADAMS/View model and above mentioned 5 DOF half car model has identical dimensions, mass, stiffness and damping properties. To give excitations due to speed hump on front and rear axle ADAMS/View motion command is used. All the assumptions made in 5 DOF half car model are also applicable to this model.

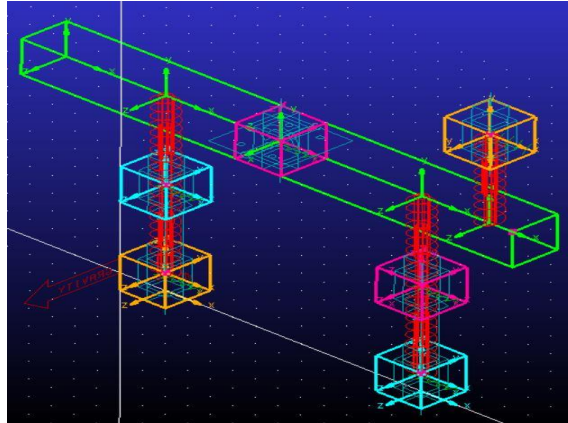
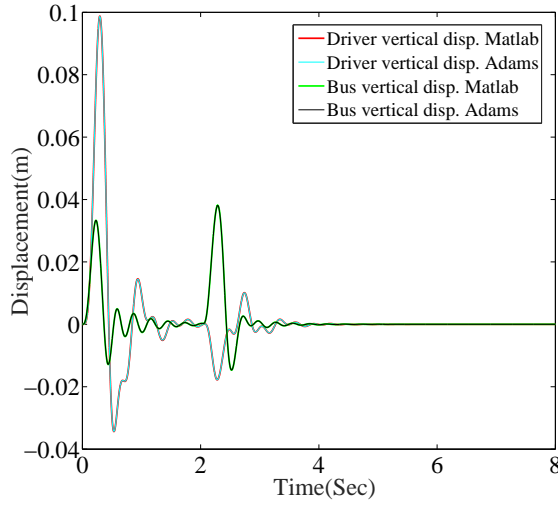


Figure 3.14: 5 DOF Half Car Model in ADAMS

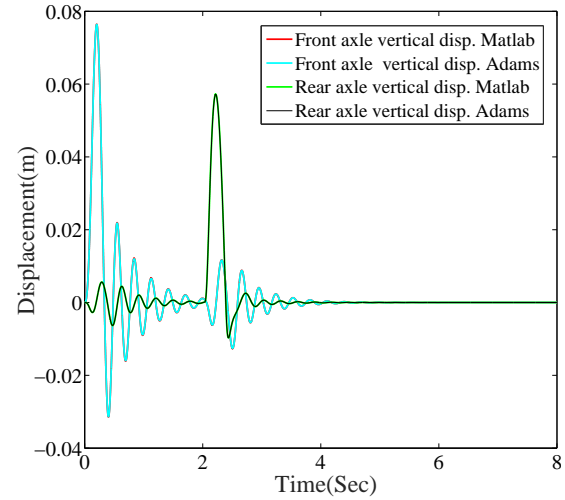
3.8 Validation of 5 DOF model with ADAMS

To validate 5 DOF half car model with ADAMS/View, numerical solving of the differential equations of motion of 5 DOF half car model is done through the program written in MATLAB and MATLAB's 'ode45' function is used for that. To simulate half car model in ADAMS/View GSTIFF solver is used. Excitation on front and rear axle in both the models are same and is describe by rounded profile speed hump. The time of simulation is limited to 8 seconds for both the MATLAB and ADAMS/View simulation.

All validation's are carried out by giving constant velocity 10 km/h to the vehicle.



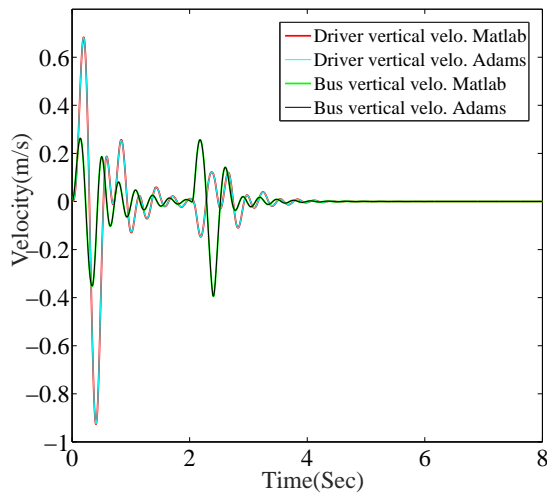
(a) Displacement(m) Vs Time(Sec)



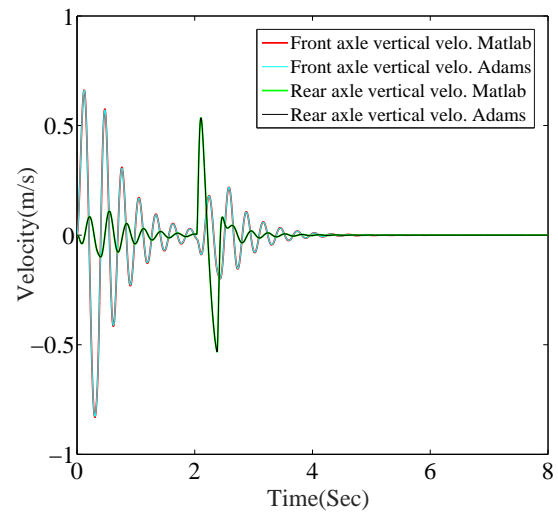
(b) Driver Displacement(m) Vs Time(Sec)

Figure 3.15: Validation of displacement while passing over Rounded Profile

Figure 3.15 and figure 3.16 shows comparison of displacement and velocity for driver, bus, front axle and rear axle. From figure 3.15 and figure 3.16, it is clear that displacement and velocity of both MATLAB and ADAMS/View models exactly matching.



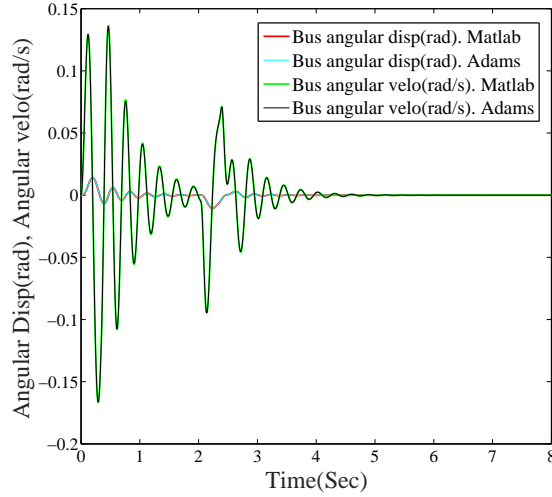
(a) Velocity(m/s) Vs Time(Sec)



(b) Velocity (m/s) Vs Time(Sec)

Figure 3.16: Validation of velocity while passing over Rounded Profile

Figure 3.17 shows comparison of angular displacement (pitching) and angular velocity (pitch velocity) for bus. From figure 3.17 it is clear that angular displacement and angular velocity of both MATLAB and ADAMS/View models exactly matching.

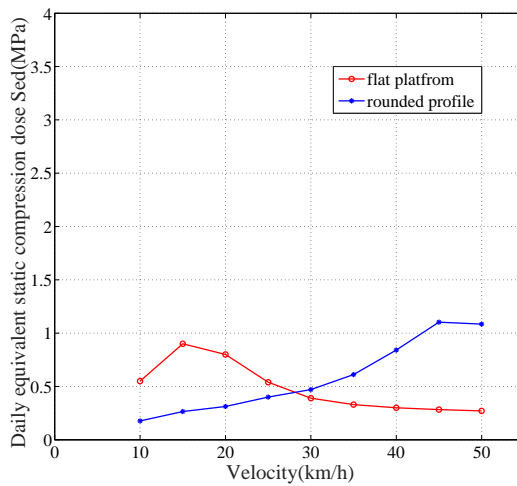


(a) Angular displacement(rad), Angular Velocity(rad/s)
Vs Time(Sec)

Figure 3.17: Validation of angular displacement and angular velocity while passing over Rounded Profile

3.9 Daily equivalent static compression dose

ADAMS/View model is simulated at various speeds ranging from 10 km/h to 50 km/h and at each speed driver's seat acceleration in verical direction is recorded. This numerical data is exported from ADAMS/View post processor and saved in ASCII file with the extension .txt, and with two columns. The first column contains time data, and second column contain measured acceleration in the seat. After recording driver's seat acceleration by using annex D of ISO 2631-5:2004 daily equivalent static compression dose (S_{ed}) is calculated.



(a)

Figure 3.18: Variation of daily equivalent static compression dose with velocity for driver

Figure 3.18 shows variation of S_{ed} with speed for driver while crossing flat platform and rounded profile speed hump. For flat platform with increasing speed S_{ed} is decreasing. When speed is above 27 km/h S_{ed} for driver is below 0.5 MPa. At higher speed's the probability of negative effect of vibration on health is low.

While crossing rounded profile speed hump with increasing speed S_{ed} is increasing. When speed is above 31 km/h S_{ed} for driver is above 0.5 MPa. At higher speed's the probability of negative effect of vibration on health is high.

3.10 Summary

In this chapter two different half car models are defined. One is 6 DOF half car model which has sprung mass, two unsprung masses and two concentrated masses representing two passengers. Spring damper attached between sprung mass and unsprung mass represents suspension system of the vehicle. Another model is 5 DOF half car model where instead of two passengers one driver is there. This both models simulated in ADAMS/View and seat acceleration for passenger1, passenger2 and driver recorded. This acceleration data is exported from ADAMS/View post processor and saved with .txt extension. Using annex D of ISO 2631-5:2004 daily equivalent static compressive dose is calculated.

To investigate effect of seat inclination on daily equivalent static compression dose, similar 6 DOF inclined halfcar model is built in ADAMS/View. With increase in seat inclination daily equivalent static compression dose decrease. Rear seated passenger experiences more discomfort than middle seated passenger.

Chapter 4

Human Body model and Analysis

4.1 Introduction to human body

Figure 4.1 shows multibody model of human body. Multibody model of human body consist of rigid bodies which represents major human body parts and structured as a linked open-tree multibody system. This model has major 6 segments namely: Head and Neck, Upper leg, lower leg, Arm, Forearm and Thorax consists of five lumbar vertebrae (L1-L5), twelve thoracic vertebrae (T1-T12), sacral spine(S1-S2) and coccygeal vertebrae. Two adjacent segments are connected by revolute joint, there are total 5 revolute joints in this model namely: Neck joint which connects Hrad Neck and Thorax joint, Shoulder joint between arm and thorax, Hip joint between thorax and upper leg, Knee joint between upper leg and lower leg, Elbow joint between arm and forearm. To consider Soft tissues, ligaments and muscles, at each revolute joint this model consist of torsional spring damper.

Detaile multibody model of human body is given in [10]. The basic data for this human body segmentation is taken from Robbins [11] technical report on “Anthropometry of motor vehicle occupants”. In which 50th percentile human male body anthropometry and mass distribution is given. This human body model represents driver in combined vehicle and human body model.

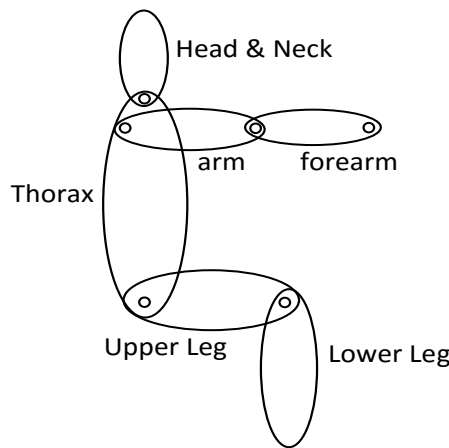


Figure 4.1: Multibody model of human body

4.1.1 Human body parameters

The mass distribution for various segments of human body model is given in table 4.1. The predicted average masses for the segments of a 50th percentile male are taken from Schneider [12]. Stiffness and damping parameters of torsional spring damper given in table 4.2. These values are assumed after the relevant literature (Cho-Chung LIANG and Chi-Feng CHIANG; 2007) [9].

Body segment	Mass	
Head and Neck	5.5	kg
Thorax	35	kg
Upper Leg	9	kg
Lower Leg	5	kg
Upper Arm	2	kg
Lower Arm	2	kg

Table 4.1: Mass parameters of the human body

Joint	Stiffness		Damping	
Head Neck and Thorax joint	328	Nm/rad	724	Nm/(rad/s)
Shoulder joint	915	Nm/rad	34	Nm/(rad/s)
Hip joint	162	Nm/rad	30	Nm/(rad/s)
Knee joint	162	Nm/rad	30	Nm/(rad/s)
Elbow joint	328	Nm/rad	724	Nm/(rad/s)

Table 4.2: Torsional spring damper properties

4.2 Combined vehicle and human body model in ADAMS/View

To study joint reaction forces in human body while crossing speed hump. A combined half car and human body model is built in ADAMS/View. Figure 4.2 shows a combined half car and human body model in ADAMS/View. This model has sprung mass, front wheel, rear wheel, suspension system and driver.

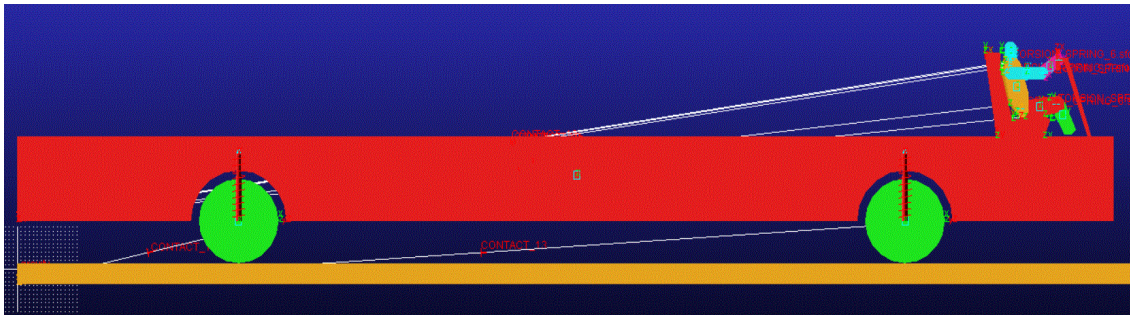


Figure 4.2: Combined vehicle and human body model in ADAMS

Driver is represented by major body segments, details of the driver model are given in previous section (4.1). Mass, Suspension and geometry parameters for half car model are given in Table 4.3 and Table 4.4. Contact between forearm and steering wheel is represented by revolute joint.

Mass parameter		Value	
m	suspended mass of the partially loaded bus	11900	kg
m_{t1}	mass of the front axle	745	kg
m_{t2}	mass of the rear axle	1355	kg
J_y	inertia moment of the suspended mass related to transversal axis	50000	kgm^2
c_p	stiffness of front axle suspension	350000	N/m
b_p	front axle shock absorbers damping	800000	Ns/m
c_z	stiffness of rear axle suspension	811250	N/m
b_z	rear axle shock absorbers damping	91265	Ns/m

Table 4.3: Mass and Suspension parameters of the bus

Geometry parameter		Value	
l	distance between axles	8.37	m
a	distance from the front axle to CG	4.12	m
b	distance from the rear axle to CG	4.25	m
r_s	distance from the driver's seat to the front axle	1.35	m
L	Total length of the vehicle	13.77	m

Table 4.4: Geometry parameters of the bus

To simulate combined half car and human body model in ADAMS/View GSTIFF solver is used. Excitation on front and rear axle are same and is describe by rounded profile speed hump. The time of simulation is limited to 13.5 seconds for this simulation. This model is simulated for two different cases as:

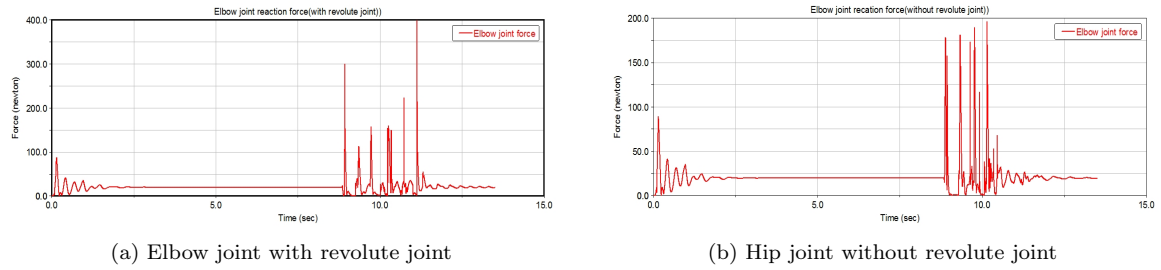
- When there is revolute joint between forearm and steering wheel, revolute joint indicates steering wheel is hold by driver tightly.
- When there is no revolute joint between forearm and steering wheel, it indicates steering wheel is hold by driver loosely.

This both simulations are carried at vehicles constant speed of 10 m/sec (36 km/h).

4.3 Comparison of joint reaction forces

Figure 4.3 shows when steering wheel is tightly hold (with revolute joint) magnitude of joint reaction force on elbow joint is high and when steering wheel is losely hold (without revolute joint) magnitude of joint reaction force on elbow joint decrease. Figure 4.4, figure 4.5. figur4.6 and

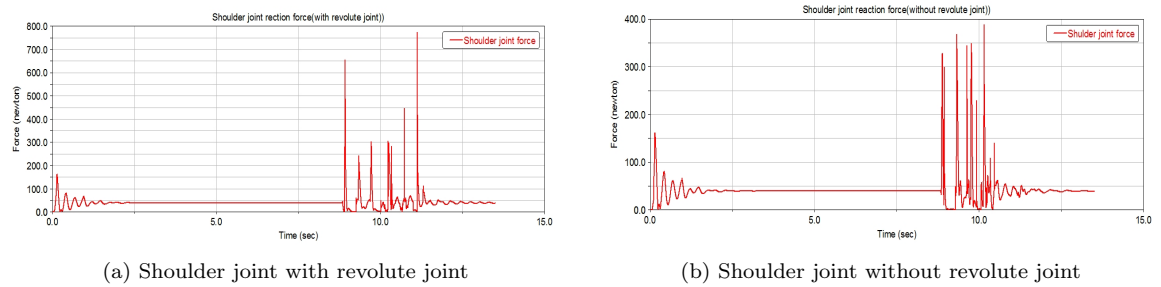
figure 4.7 shows similar results for shoulder joint, hip joint, knee joint and head neck thorax joint respectively.



(a) Elbow joint with revolute joint

(b) Hip joint without revolute joint

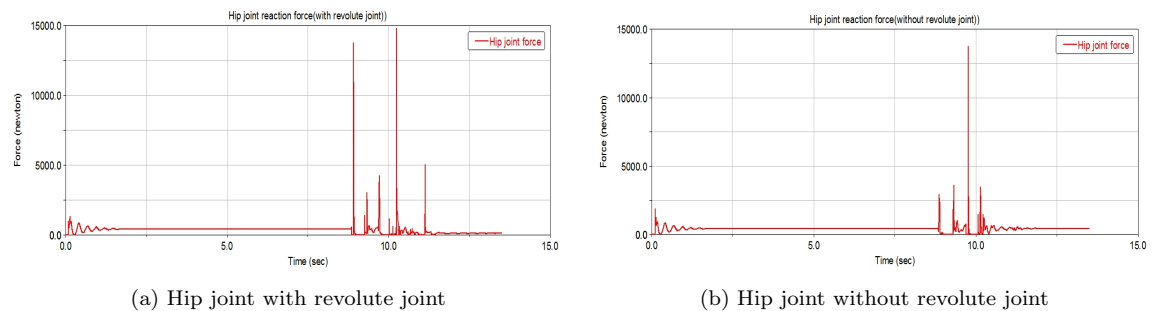
Figure 4.3: Comparison of joint reaction forces on Elbow joint



(a) Shoulder joint with revolute joint

(b) Shoulder joint without revolute joint

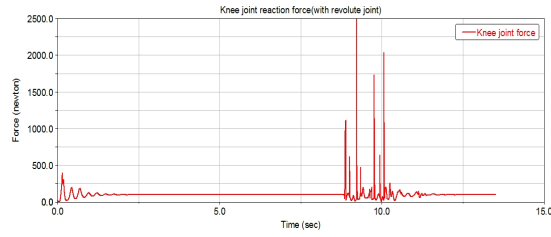
Figure 4.4: Comparison of joint reaction forces on Shoulder joint



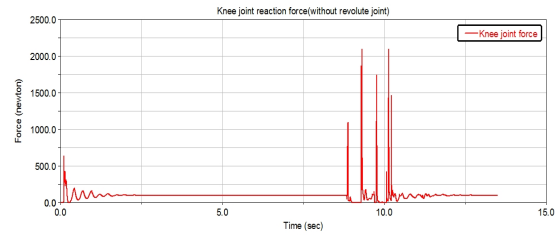
(a) Hip joint with revolute joint

(b) Hip joint without revolute joint

Figure 4.5: Comparison of joint reaction forces on Hip joint

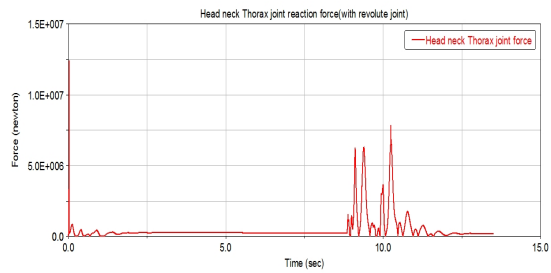


(a) Knee joint with revolute joint

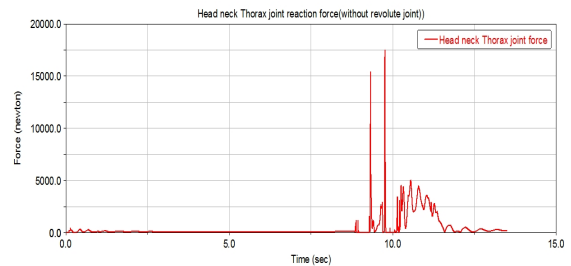


(b) Knee joint without revolute joint

Figure 4.6: Comparison of joint reaction forces on Knee joint



(a) Head Neck Thorax joint with revolute joint



(b) Head Neck Thorax joint without revolute joint

Figure 4.7: Comparison of joint reaction forces Head Neck Thorax joint

4.4 Summary

A combined multibody model of human body and half car is built in ADAMS/View. Multibody model of human body has six major segments adjacent segments are connected by revolute joint. To consider soft tissues, ligaments and muscles, at each revolute joint this model has torsional spring damper. This model is simulated in ADAMS/View for two different cases, first with revolute joint (Steering is hold tightly) between forearm and steering wheel and second without revolute joint (Steering is hold loosely) between forearm and steering wheel. Joint reaction forces at joint for both the simulation calculated. On comparing this forces it came to know that without revolute joint (steering is hold loosely) magnitude of reaction forces at each joint less compared to within revolute joint (Steering is hold tightly) simulation.

Chapter 5

Conclusions and Recommendations

5.1 Conclusions

For passengers with increase in seat inclination acceleration along vertical direction decreases and passenger feels more comfortable, also with increase in seat inclination daily equivalent static compression dose (S_{ed}) reduces significantly. So to reduce adverse effect of whole body vibration on human body proper seat inclination is to be given. Parameter S_{ed} varies with speed of the vehicle, at higher speeds parameter S_{ed} crosses both the assessment criteria, so the probability of negative effect of vibrations to health is significant. Compare to flat platform speed hump, while crossing rounded profile speed hump has high value of S_{ed} . Rear end seated passenger experiences more discomfort than middle seated passenger. While crossing speed hump, on the health of rear end seated passenger has adverse effect.

To increase driver's seat inclination we have some limitation, because driver's seat can not be inclined more than 10 degrees. For driver to reduce magnitude of joint reaction forces, while passing over the speed hump the driver should loosen his grip over steering wheel.

5.2 Recommendations

With seat inclination S_{ed} reduces significantly, so to improve passenger comfort seat inclination has to be given importance while designing vehicle. Compare to rounded profile speed hump, flat platform speed humps are recommended in view of passenger safety and comfort. Driver should slow down when about to cross speed hump. While crossing speed hump the driver should loosen the grip over steering wheel. Half car model is similar to bicycle model so all the above results are applicable to bicycle model.

In this model we didn't consider seat stiffness, by adding seat stiffness in the model peak joint reaction forces in the human body may be reduced. If we consider stiffness of the seat, seat stiffness reduces amplitude of vertical acceleration experienced by driver and increases driver's riding comfort. So while passing over speed hump peak joint reaction forces in the human body may be reduced.

Bibliography

- [1] D. R. Smith and P. A. Leggat. Whole-Body Vibration. *Professional safety* 50, (2005) 35.
- [2] W. De Craecker, H. Druyts, H. Ramon, E. Forausbergher, B. Haex, R. Van Audekercke, P. Coorevits, and G. Vanderstraeten. Investigation of the Effect of Whole-Body Vibration on the Human Body by Spine Modelling. Technical Report, SAE Technical Paper 2005.
- [3] S. Tabacu, N. Pandrea, N. D. Stanescu, N. Mastorakis, A. Croitoru, V. Balas, E. Son, and V. Mladenov. A Seven Degrees of Freedom(7 DOF) Human Body- Vehicle Structure Model for Impact Applications. In WSEAS International Conference. Proceedings. Mathematics and Computers in Science and Engineering, 10. World Scientific and Engineering Academy and Society, 2009 .
- [4] V. Dedović and D. Sekulić. Effect of shock vibrations due to speed control humps to the health of city bus passengers using oscillatory model with six DOF. In International Conference on Traffic and Transport Engineering-Belgrade. 2012 .
- [5] W. Abbas, A. Emam, S. Badran, M. Shebl, and O. Abouelatta. Optimal Seat and Suspension Design for a Half-Car with Driver Model Using Genetic Algorithm. *Intelligent Control and Automation* 4, (2013) 199.
- [6] W. Abbas, O. B. Abouelatta, M. El-Azab, M. Elsaidy, A. A. Megahed et al. Optimization of biodynamic seated human models using genetic algorithms. *Engineering* 2, (2010) 710.
- [7] C.-C. Liang and C.-F. Chiang. A study on biodynamic models of seated human subjects exposed to vertical vibration. *International Journal of Industrial Ergonomics* 36, (2006) 869–890.
- [8] L. Johnson and A. Nedzesky. A comparative study of speed humps, speed slots and speed cushions. In ITE Annual Meeting Compendium, Institute of Transportation Engineers (ITE), Washington, DC. 2004 .
- [9] D. Sekulić, V. Dedović, and S. Rusov. Effect of shock vibrations due to speed control humps to the health of city bus drivers. *Scientific Research and Essays* 7, (2012) 573–585.
- [10] L. Hynčík and H. Čechová. Car impact to pedestrian—fast 2D numerical analysis. *Applied and Computational Mechanics* 5.
- [11] D. Robbins, L. W. Schneider, R. Snyder, M. Pflug, and M. Haffner. Seated posture of vehicle occupants. Technical Report, SAE Technical Paper 1983.

- [12] T. Shams, T. Huang, N. Rangarajan, and M. Haffner. Design requirements for a fifth percentile female version of the THOR ATD. In 18th International Technical Conference on the Enhanced Safety of Vehicles, Nagoya, Japan. 2003 19–22.
- [13] ISO 2631-5:2004 Mechanical vibration and shock – Evaluation of human exposure to whole-body vibration – Part 5: Method for evaluation of vibration containing multiple shocks.